Numerical study of the fluid-structure interaction of composite hydrofoil with different plying angles in steady flow

H Z Zhang[1], Q Wu[2], B Huang[1*] and G Y Wang[1]

[1] School of Mechanical Engineering, Beijing Institute of Technology, Beijing, China
[2] Department of Thermal Engineering, Tsinghua University, Beijing, China

* huangbiao@bit.edu.cn

Abstract. The object of this paper is to numerically investigate the fluid-structure interaction of composite hydrofoil. The aim is to validate 3D numerical simulation model with fluid-structure interaction of composite materials comparing to experimental data, and study the fluid-structure interaction of composite hydrofoil. Numerical results are presented for a composite hydrofoil. The hydrofoil has unswept trapezoidal planform of aspect ratio 3.33. The numerical model has been validated and showed reasonable agreement with the experiment measurements. Then the forces and deformations of composite hydrofoil with different plying angles have been investigated at Re=1x10^6 and initial angle of attack α=6º. The results show that lift and drag coefficients and tip twist angle decrease and get minimum at about plying angle θ=35º. According to Classical Laminate Theory, the intrinsic bending-twisting coupling of composite structures leads to the variation of twist angle for different plying angles. The relation expression on elements of matrices D has been derived to estimate twist angle at tip qualitatively.

1. Introduction

For maritime transport, nowadays it has difficulties in continuing to improve its performance and fuel efficiency with traditional design methods on metallic materials. Composite materials have been applied to marine due to its great advantages such as higher strength-to-weight ratios and improved vibration damping properties [1-3]. However due to the density of water is larger than that in air, the structural response under water becomes more complex with intrinsic coupling behaviors. Therefore, the influence of intrinsic coupling behaviors on fluid-structure interaction has been extremely needed to investigated. The objective of this paper is to validate 3D numerical model with fluid-structure interaction(FSI) comparing to experiments [4] and study the fluid-structure interaction of composite hydrofoil.

2. Numerical model

2.1. Solid model

The geometry of hydrofoil has unswept trapezoidal planform with 0.3m span,0.12m base chord, and 0.06 m tip chord as shown in figure 1.

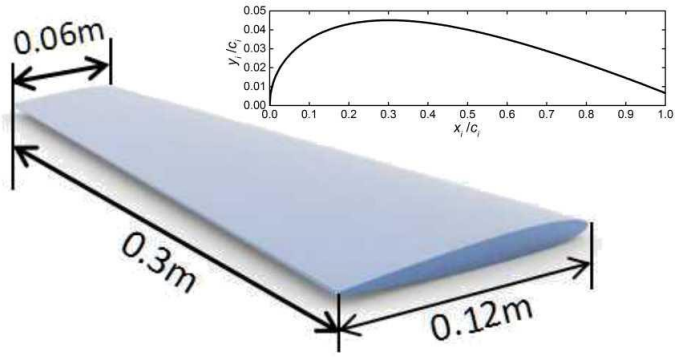

Figure 1. Schematic of geometry of trapezoidal hydrofoil with modified NACA0009 section profile.

The layers of the composite hydrofoil, which are in accordance with Zarruk et al[4], are mixed with carbon fabrics and three kinds of E-glass fabrics. The stacking sequence of hydrofoil is $[(0^o/90^o)_{g\text{-}basket},(0^o/90^o)_{g\text{-}biaxial}, (\theta)_{5c}, (0^o/90^o)_{2g\text{-}biaxial}, (\theta)_{4c}]_S$ with one glass-mat layer in the center of the hydrofoil, where the subscript g and c represent glass fabric and carbon fabric respectively, the subscript S means that the layers is symmetrical about the mid-plan, and the θ refers to the angle between axes of carbon fabrics and local axes, are shown in figure 2.

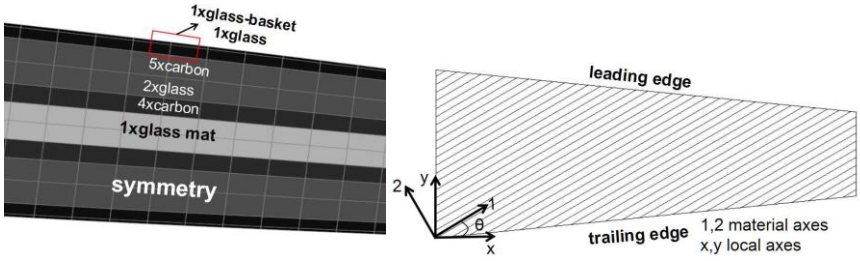

(a) (b)

Figure 2. (a)The stacking sequence of hydrofoil (b)Planform view of hydrofoil with material and local coordinate systems

2.2. Fluid model

The fluid domain is consistent with experimental tunnel whose section is 0.6m square by 2.6m long, where the hydrofoil is located at the 0.7m from the entrance. The boundary conditions of the 3-D fluid domain is shown in figure 3. The fluid domain is solved by incompressible and steady Reynolds Average Navier-Stokes equations with *k-ω* SST turbulence model[5].

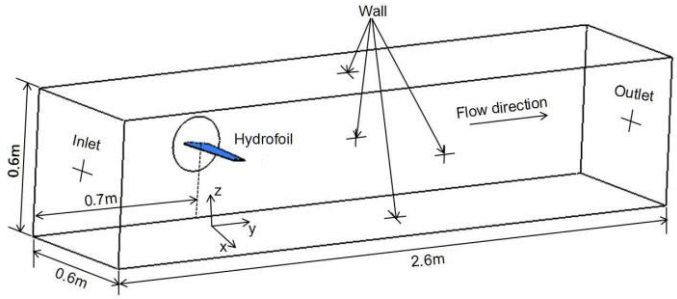

Figure 3. Boundary conditions of fluid domain with global coordinates.

2.3. FSI coupling modelling

Figure 4 shows the flow chart of the FSI coupling algorithm used in this paper. Firstly, the Structure Solver solves solid structure deformation with applied loads from CFD Solver in the previous time /iteration step or initialization. Then the CFD Solver, commercial software CFX, updates mesh of fluid domain with the before solved deformation, solves flow fields and gets force of hydrofoil to transfer to Structure Solver. When the finish criterion is satisfied, the whole solving process finishes.

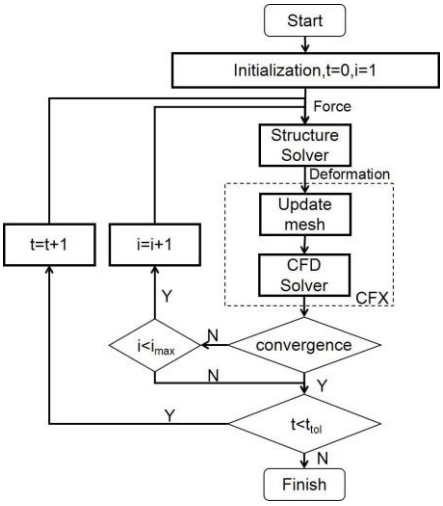

Figure 4. Coupling algorithm of Fluid-Solid Interaction

3. Results and discussion

3.1. Numerical validations

The predicted lift coefficients $C_L = 2L/(\rho_L U_\infty^2 sc)$ and drag coefficients $C_D = 2D/(\rho_L U_\infty^2 sc)$ for two Reynolds numbers($Re=U_\infty c/\nu_f$) with different initial angles of attack(α_0) at plying angle θ=0º are compared to the experiments, as shown in figure 5, where L, D, U_∞, c and s, refer to lift, drag, free stream velocity, mean chord (c=0.09 m) and hydrofoil span(s=0.3 m) respectively.

The evolution tendency of lift and drag coefficients is consistent with experiment. As initial attack of angle increases, both lift and drag coefficients experience an increase. With Reynolds number increasing, the lift coefficient has same trend with Reynolds number, which is in opposed to drag coefficient.

Figure 6 shows twist angles(β) at tip compared with experimental results for two plying angles(θ) with different initial angles of attack(α) at Re = 1x10^6. The twist angle at tip for two plying angles shows agreement with experimental results that twist angle at tip is negative at θ=30º in opposed to positive twist angle at θ=0º.

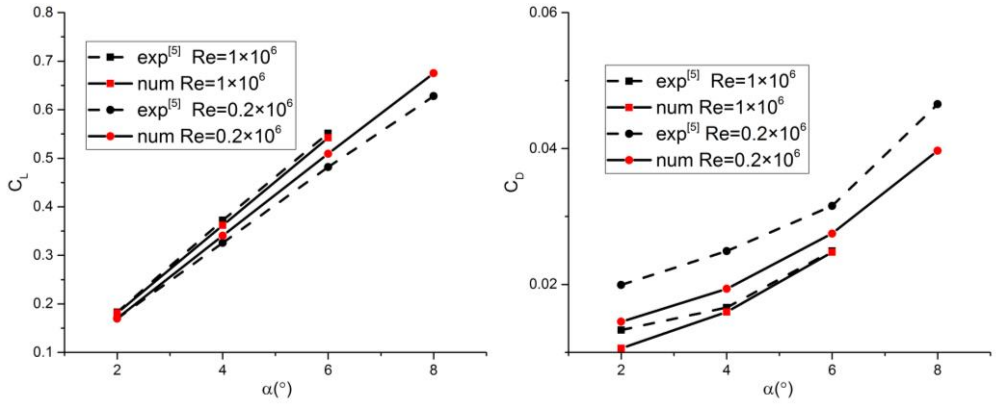

(a) (b)

Figure 5. Comparison of lift coefficient(C_L),drag coefficient(C_D) for two Reynolds numbers(Re) with several initial angles of attack(α) at θ=0º.(a)lift coefficient (b)drag coefficient.

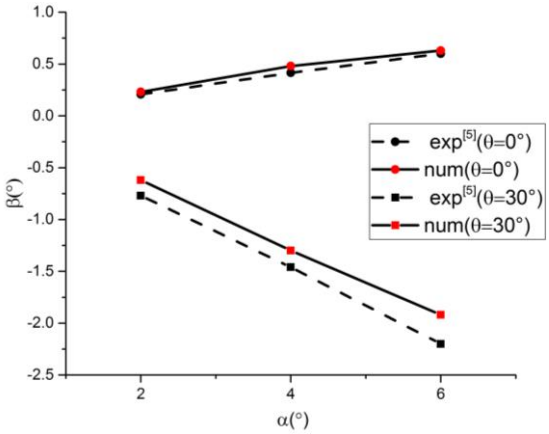

Figure 6. Comparison of twist angle(β) at tip for two plying angle(θ=0° and θ=30°) with different initial angles of attack(α) at Re=1x10^6.

As described above, the numerical model can be employed to study the influence on performance, deformation and flow pattern of different plying angles. This paper focus on the intrinsic coupling effects of composite materials on different plying angle rather than variation of Reynolds numbers or initial incidence. Hence, following conditions are set at Re = 1x10^6 and α=6º with different plying angles.

3.2. The fluid-structure interaction of composite hydrofoil

Figure 7 shows the dimensionless coefficients and tip twist angle with plying angle for Re=1x10^6 and α=6º. As plying angle increases from θ=0º, the lift and drag coefficients decrease and get minimum at about θ=35º and then increase. The evolution tendency of twist angle at tip is consistent with the dimensionless coefficients. Twist angle influences angle of attack, which plays a significant role in performance coefficients. The intrinsic coupling effects causes different tip twist angle. Thus it is necessary for design of composite structure to find out the relationship between twist angle and intrinsic coupling effects.

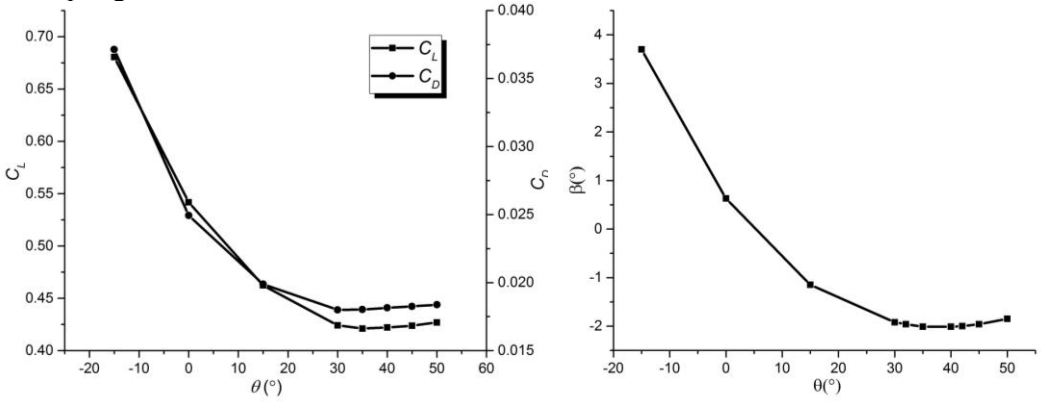

(a) (b)

Figure 7. Lift and drag coefficients and tip twist angle with plying angle for Re=1x106 and α0=6 º .(a)lift and drag coefficients. (b) tip twist angle.

Due to thickness of the composite hydrofoil in this paper is much smaller than the length of chord and span, the solid model can be regarded as laminate and the influence of shape can be ignored tentatively. Then the classical laminate theory(CLT)[6] can be employed to represent intrinsic coupling behavior with different plying angles. In CLT, the midplane twist curvatures κ_{xy} represents twist of laminate, which can be chosen to represent twist angle qualitatively although the dimension is not unified. The definition of midplane twist curvature in CLT is shown as:

$$\kappa_{xy} = -2\frac{\partial^2 \omega_0}{\partial x \partial y} \tag{1}$$

where ω_0 represents the displacement of composite hydrofoil in global z direction. Due to the actual solid model is not laminate, the average twist curvature $\overline{\kappa}_{xy}$ is adopted to represent midplane twist curvature in CLT. The comparison between tip twist angle and average twist curvature is shown in figure 8. The trend of variation is consistent with each other.

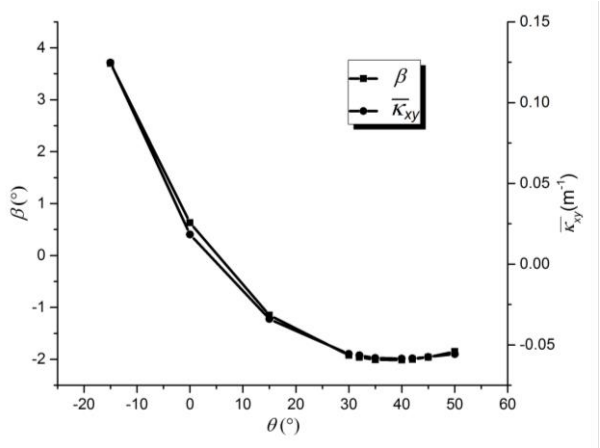

Figure 8. Tip twist angle and average twist curvature with different plying angles

The structure can be considered as a symmetric laminate, which causes the B_{ij}=0 and all the elements in the matrices A and D would be present. Therefore, the laminate exists extension-shear coupling and bending-twisting coupling resulted in by A and D respectively. In this paper, the bending-twisting coupling, which is due to existence of D_{16} and D_{26}, is investigated primarily.

Thus the midplane twist curvature can be written as:

$$\kappa_{xy} = \varepsilon M_x + \gamma M_y + \lambda M_{xy} \tag{2}$$

where M_x, M_y and M_{xy} are internal moment in x and y directions and internal torque per unit width respectively, and the definitions of coefficients ε, γ and λ are shown as below:

$$\varepsilon = \frac{(D_{16}D_{22} - D_{12}D_{26})}{D_{66}D_{12}^2 - 2D_{12}D_{16}D_{26} + D_{22}D_{16}^2 + D_{11}D_{26}^2 - D_{11}D_{22}D_{66}} \tag{3}$$

$$\gamma = \frac{(D_{11}D_{26} - D_{12}D_{16})}{D_{66}D_{12}^2 - 2D_{12}D_{16}D_{26} + D_{22}D_{16}^2 + D_{11}D_{26}^2 - D_{11}D_{22}D_{66}} \tag{4}$$

$$\lambda = \frac{(D_{12}D_{12} - D_{11}D_{22})}{D_{66}D_{12}^2 - 2D_{12}D_{16}D_{26} + D_{22}D_{16}^2 + D_{11}D_{26}^2 - D_{11}D_{22}D_{66}} \tag{5}$$

According to equation (2), the κ_{xy} is mainly determined by ε, γ, and λ for similar forces. And ε, γ, and λ are calculate from material properties, layer thickness and stacking sequence of the layers. Thus it can be employed to predict twist angle of structure under different material properties or plying angles, and offer help to the design of marine propulsors.

References

[1] Mouritz, A., Gellert, E., Burchill, P., and Challis, K., 2001. Review of advanced composite structures for naval ships and submarines. Composite Structures, 53, pp. 21–41.
[2] Glaz B, Friedmann P P, Liu L. Helicopter Vibration Reduction throughout the Entire Flight Envelope Using Surrogate‐Based Optimization[J]. Journal of the American Helicopter Society, 2009, volume 54(1):12007.
[3] Krone, N. J. Divergence Elimination with Advanced Composites. AIAA Paper 75-1009.
[4] Zarruk,Gustavo A., et al. "Experimental study of the steady fluid–structure interaction of flexible hydrofoils." Journal of Fluids & Structures 51(2014):326-343.
[5] Menter, F.R.,1993.Improved two-equation k omega turbulence models for aerodynamic flows.NASATechnicalMemorandum103975,34.More references
[6] R.M. JONES, "Mechanics of Composite Materials" (Hemisphere,New York, 1975) pp. 154, 214.